ECLÉTICA QUÍMICA

Eclet. Quim. 51 | e-1621, 2026

Original Article

https://doi.org/10.26850/1678-4618.eq.v51.2026.e1621

# Efficient nano-preparation, characterization, and biological evaluation of two Schiff base-derived complexes

Ahmed Ali **Qaid**[1], Sadeq Hamood **Azzam**[1], Amani Ahmed **Al-Gaadb**[1], Bushra Mohammed **Alattab**[1], Fares Abdullah **Alarbagi**[1,2], Mohammed Kassem **Al-qadasy**[1], Saad Abdullah **Al-Arnoot**[3], Maher Ali **Al-Maqtari**[1+]

## Abstract

**This study aims to prepare a new Schiff base, 2-[(E)-[2-(2,4-dinitrophenyl)hydrazinylidene]methyl]-1H-pyrrole (NPHP), derived from 2,4-dinitrophenyl hydrazine and 1H-pyrrole-2-carbaldehyde with ratio 1:1. Additionally, two new complexes of this Schiff base were synthesized with transition metal ions, Ni(II) and Cu(II), with ligand to metal ratio 2:1. The complexes were characterized using molar conductivity, FT-IR, UV-Vis, $^{1}$HNMR, $^{13}$CNMR, XRD, and transmission electron microscopy. Physicochemical properties and spectral results indicate that the conductivity showed an electrolytic nature for these complexes, and the ligand acts as a bidentate chelating agent with octahedral geometry, as supported by FT-IR and UV-Vis analysis. The azomethine (CH=N) nitrogen and pyrrole nitrogen atoms were identified as the coordination sites. Pathogenic bacterial studies for the ligand and its new complexes, Ni(II) and Cu(II), were conducted against *Escherichia coli*, *Staphylococcus aureus*, and *Pseudomonas aeruginosa*. Based on chelation theory, the metal complexes exhibited higher biological activity than the free ligand, while the complex of Ni(II) was more effective than the complex of Cu(II). Notably, the Schiff base (NPHP) showed no activity against *Escherichia coli*.**

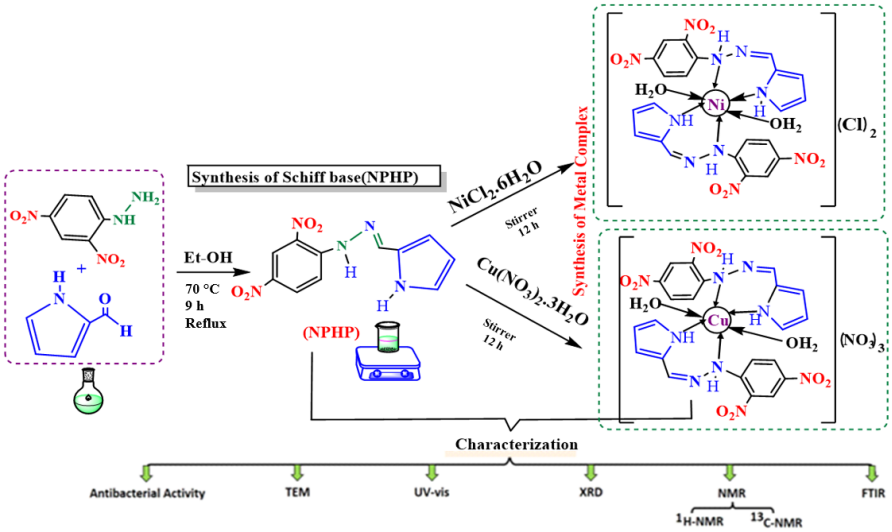


## Article History

| | |
|---|---|
| **Received** | January 31, 2025 |
| **Accepted** | April 06, 2025 |
| **Published** | April 06, 2026 |

## Keywords

1. new transition metal complex
2. Schiff base
3. antibacterial activity
4. spectral Analysis
5. metals ions.

## Section Editors

Manuel Ignacio Azocar Guzmán

## Highlights

- Preparation of the Schiff base as a new ligand.
- Preparation of transition metal complexes with ligands for both nickel and copper.
- Study of the physical properties of the prepared ligands and complexes.
- Conducting spectroscopic analyzes of ligands and their complexes.
- Prepared ligand and its complexes effectiveness against some microorganisms.

[1]Sana'a University, Chemistry Department, Sana'a, Yemen. [2]Amarn University, Pharmacy Department, Amran, Yemen. [3]Sana'a University, Biological Department, Sana'a, Yemen. **+Corresponding author:** Maher Ali Almaqtari, **Phone:** +967773262252, **Email address:** m.almaqtari@su.edu.ye

https://doi.org/10.26850/1678-4618.eq.v51.2026.e1621

# 1. Introduction

Heterocyclic compounds show significant efficacy against bacterial and viral pathogens by targeting the respiratory chain cells (Suman *et al.*, 2017). Many derivatives of heterocyclic compounds also possess remarkable organic and pharmacological properties, which makes them valuable in pharmaceutical applications (Kashaw *et al.*, 2008). As for the Schiff bases, formed by the reaction of amino and carbonyl as aldehydes or ketones compounds and replacing the carbonyl group (C=O) with an imine (C=N) or an azomethine group, Schiff bases act as effective chelating agents when they contain coordinated functional groups (Mushtaq *et al.*, 2024; Yousif *et al.*, 2017). Schiff bases and their metal complexes play a key role in understanding the coordination chemistry of transition metal ions (Yilmaz *et al.*, 2009). Schiff base metal complexes containing different metal ions such as Ni, Co, and Cu have been studied in detail for their various crystallographic features, structure-redox relationships, enzymatic reactions, mesogenic characteristics, and catalytic properties (Kilic *et al.*, 2012)

Schiff bases can be strengthened by improving their biological effectiveness (Ragi *et al.*, 2021; Al Zoubi *et al.*, 2016). With donor groups (Bhaskar *et al.*, 2020). Schiff bases coordinate with metal ions through azomethine nitrogen and have been extensively studied (Aalami *et al.*, 2024). The binding (C=N) in azomethine derivatives is vital for their biological activity, contributing to antifungal, antibacterial, anticancer and antimalarial effects (Shivankar *et al.*, 2003).

A lot of important literature surveys witnessed a great deal of interest in the synthesis and characterization of transition metal complexes containing Schiff bases as ligands due to their applications in asymmetric catalysis, materials science, analytical, and medicinal chemistry and possess intrinsic pharmacological properties (Alhafez *et al.*, 2022; De *et al.*, 2022; Kilic *et al.*, 2012; Ilhan *et al.*, 2008). It also has applications in industrial processes, laboratory settings, dye manufacturing, corrosion inhibition, drug synthesis, catalysis, coordination chemistry, and the study of biological agents (Ceramella *et al.*, 2022).

Nanoparticles, ranging from 1 to 100 nm in diameter, are one-dimensional materials that possess unique properties and a wide range of applications, particularly in pharmaceuticals and medicine (Altammar, 2023; Prabhu and Poulose, 2012). They represent alternative antibacterial agents by their ability to interact with bacterial cells by disrupting membranes or inhibiting enzyme activity (Ahmed *et al.*, 2019; Hezam *et al.*, 2019).

The field of nano complexes has had a significant impact on inorganic chemistry, particularly in pharmaceuticals and medicine (Al-Maqtari *et al.*, 2023; Prabhu and Poulose, 2012).

Therefore, this study aims to synthesize a Schiff base from (2,4-dinitrophenyl) hydrazine and 1-pyrrole-2-carbaldehyde, followed by the preparation of coordination compounds with Ni (II) and Cu(II) salts as nanoparticle products. Characterization of these compounds will be carried out using FTIR, UV-Vis, $^{1}$H NMR, $^{13}$C NMR, XRD, TEM, and antibacterial activity.

# 2. Materials and methods

## 2.1. Materials

All chemicals were used as received without further purification. The Schiff base precursors, pyrrole-2-carboxaldehyde (99% purity, Fluka) and 2,4-dinitrophenyl hydrazine (98% purity, Scharlau), were employed for ligand synthesis. Metal salts, including nickel (II) chloride hexahydrate ($NiCl_2{\cdot}6H_2O$, 99% purity, Scharlau) and copper(II) nitrate hexahydrate ($Cu(NO_3)_2{\cdot}6H_2O$, 99% purity, Scharlau), were utilized for complexation. The solvents dimethyl sulfoxide (DMSO, 99.8% purity, Scharlau) and absolute ethanol 99.8% purity, Sigma-Aldrich) served as reaction media and for purification purposes. All reagents were of analytical grade to ensure the reliability of experimental outcomes.

## 2.2. Methods

### 2.2.1. Preparation of Schiff base

The Schiff base ligand, 2-[(E)-[2-(2,4-dinitrophenyl) hydrazinylidene] methyl]-1H-pyrrole (NPHP), was synthesized through a condensation reaction. Specifically, 0.99 g (5 mmol) of 2,4-dinitrophenyl hydrazine was dissolved in 25 mL of absolute ethanol and then added to 0.47 g (5 mmol) of the chemical compound 1H-pyrrole-2-carbaldehyde. Additionally, 5 drops of glacial acetic acid were included as a catalyst. The mixture was refluxed for 9 h at 70 °C until a red precipitate formed, which was then recrystallized using cooled ethanol (**Scheme 1**) (Kumar *et al.*, 2009).

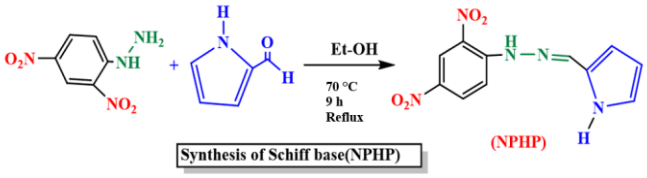


**Scheme 1.** Preparation of NPHP.
**Source**: Elaborated by the authors.

### 2.2.2. Preparation of transition metal complexes as nanoparticles

To prepare transition metal complexes, 0.12 g (3 mmol) of NaOH and 0.22 g (4 mmol) of NPHP were added to 30 mL of ethanol. This mixture was combined with a metal salt (2 mmol), specifically $NiCl_2{\cdot}6H_2O$ or Cu $(NO_3)_2{\cdot}3H_2O$, which had been dissolved in a minimal amount of distilled water. The reaction was stirred for 12 h to facilitate the complete formation of the complex. NaOH served as a precipitation agent. The resulting precipitate was filtered, washed several times with ethanol, and then dried at room temperature, producing a light brown powder (**Scheme 2**) (El-Shafiy *et al.*, 2017).

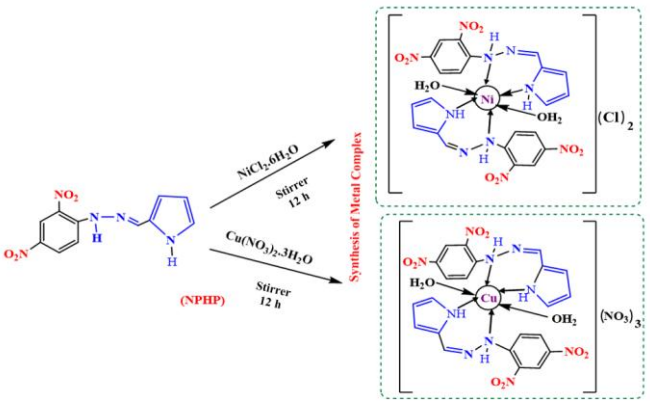


**Scheme 2.** Preparation of Ni(II) and Cu(II) complexes.
**Source**: Elaborated by the authors.

## 2.3. Characterization techniques

### 2.3.1. Physical properties

A standardized conductivity and melting point apparatus was used to determine the conductivity and melting points of the Schiff base and its metal complexes.

### 2.3.2. FT-IR spectra

FT-IR spectra were obtained using a Varian IR Prestige-2000 FT-IR spectrophotometer at the University of Science and Technology in Sana'a, Yemen.

### 2.3.3. UV-Vis spectra

The electronic spectra of the ligand and its complexes were recorded using a Cary 50 Conc UV-Visible spectrophotometer (Varian Australia) at room temperature over the wavelength range of 200–900 nm. This measurement was conducted at the Global Pharmaceuticals Company in Sana'a, Yemen.

### 2.3.4. X-ray diffraction

The crystallinity of the prepared Schiff base ligand and its Ni(II) and Cu(II) complexes was analyzed using an XD-2 X-ray diffractometer (Cu Kα, λ = 1.54 Å, 36 kV, 20 mA) at the Yemeni Geological Survey and Minerals Resources Board (YGSMRB).

### 2.3.5. NMR spectra

The $^{1}$H-NMR and $^{13}$C-NMR spectra were recorded in DMSO-$d_6$ using either a Bruker AVANCE II 300DRX or an average 400DRX spectrometer. This analysis was conducted at the Faculty of Science, Cairo University, Egypt, which is equipped with advanced NMR facilities suitable for such spectroscopic studies.

### 2.3.6. TEM analysis

A drop of the nanoparticle solution was placed on carbon-coated copper grids and allowed them to evaporate. Transmission electron microscopy (TEM) measurements were conducted using a Philips CM200 instrument, operating at an accelerating voltage of 200 kV. This analysis took place at Cairo University, Egypt.

### 2.3.7. Antibacterial activity

Antibacterial tests were performed at the Department of Microbiology, Sana'a University, Faculty of Sciences, using the standard disc diffusion method. The Schiff base ligand and its complexes were tested at concentrations of 50-100 mg/mL, dissolved in dimethyl sulfoxide (DMSO).

Cultures were incubated for 24 h at 37 °C for bacteria and 120 h for Candida. The results were recorded as the average diameter of the inhibition zone in millimeters. Microorganisms isolated from human patients included both gram-positive and gram-negative strains, including *Staphylococcus aureus*, *Pseudomonas aeruginosa*, and *Escherichia coli*.

**The methodology was as follows:**

1. **Isolation of cultures**: Microorganisms were isolated and cultured on nutrient agar medium in sterile 9-cm Petri dishes.
2. **Incubation**: The plates were incubated at 37 °C for 24 h to allow for growth.
3. **Preparation of inoculum**: A 0.5 cm diameter disc was transferred from the growth colonies of *Staphylococcus aureus*, *Pseudomonas aeruginosa*, and *Escherichia coli* into test tubes containing 10 mL of nutrient broth. The tubes were then incubated at 37 °C for 24 h.
4. **Preparation of agar plates**: Fresh nutrient agar medium was prepared and poured into sterile Petri dishes.
5. **Transfer of Cultures**: After incubation, the growth colonies from the broth were transferred into a sterile test tube and diluted as necessary for even distribution on the nutrient agar.
6. **Application of discs**: Discs saturated with the Schiff base ligand and its metal complexes were placed onto the surface of the agar.
7. **Incubation of plates**: The culture plates were incubated at 37 °C for another 24 h to allow for interaction between the compounds and the microorganisms.
8. **Measurement of inhibition zones**: After incubation, the average diameter of the inhibition zones around each disc was measured in millimeters for all tested compounds.
9. **Repetition for additional concentration**: All procedures were repeated using additional concentrations of the Schiff base ligand and its complexes to assess their antibacterial effectiveness.
10. **Sterile conditions**: All manipulations were conducted under sterile conditions to prevent contamination and ensure the reliability of the results.

# 3. Results and discussion

## 3.1. of the prepared Schiff base and its Ni(II) and Cu(II) complexes

The Schiff base and its metal (II) complexes were prepared with good yields, and their properties are summarized in **Table 1**. The Schiff base exhibits a melting point of 275 °C, while the decomposition temperatures of the Ni(II) and Cu(II) complexes are above 300 °C, indicating their thermal stability. This thermal stability is significant, as it suggests that the complexes can withstand higher temperatures without decomposing, making them suitable for various applications. The molar conductance values for the Ni(II) and Cu(II) complexes are 162.6 and 171.8 μS/m, respectively. These high molar conductance values suggest that the complexes are electrolytic, as noted by (Maher *et al.*, 2018).

https://doi.org/10.26850/1678-4618.eq.v51.2026.e1621

**Table 1.** Physical Properties of the Schiff base and two Metal (II) Complexes.

| Compounds | NPHP | $Ni^{II}$ complex | $Cu^{II}$ complex |
|---|---|---|---|
| Color | Red | light brown | dark brown |
| Yield % | 73 | 58 | 65 |
| M.P. (°C) | 275 | 303 | 305 |
| M.L. (µs/m) | - | 162.6 | 171.8 |

**Source**: Elaborated by the authors.

## 3.2. FT-IR spectra

The FT-IR spectra of NPHP (**Fig. 1**) exhibit stretching frequencies at 3420 $cm^{-1}$ and 3283 $cm^{-1}$, which are attributed to the N-H group, while a weak band at 3080 $cm^{-1}$ corresponds to the C-H stretching of the aromatic group. A strong band at 1625 $cm^{-1}$ is associated with the azomethine (HC=N) group (Bhaskar *et al.*, 2020). Additionally, absorption bands at 1520 $cm^{-1}$ and 1470 $cm^{-1}$ are assigned to the stretching vibrations of the C=C and C=N groups, respectively, as detailed in **Table 2**. Notably, the spectrum of NPHP displays a band for the -C=N- group at 1699 $cm^{-1}$, which shifts to a lower frequency between (1649-1656 $cm^{-1}$) in the spectra of Ni(II) and Cu(II) complexes. This shift indicates the involvement of -C=N-NH nitrogen in coordination with (Ni(II) and Cu(II)) metal ions (Turky Shamkhy, 2015).

**Table 2.** FT-IR data for prepared compounds.

| | Compounds | NPHP | $Ni^{II}$ complex | $Cu^{II}$ complex |
|---|---|---|---|---|
| Wave numbers ($cm^{-1}$) | υ (N-H) | 3420 | 3480 | 3430 |
| | υ (C-H) aryl | 3100 | 3080 | 3070 |
| | υ (HC=N) | 1625 | 1655 | 1635 |
| | υ (C=C) | 1505 | 1510 | 1510 |
| | υ M-N | ---- | 450 | 426 |

**Source**: Elaborated by the authors.

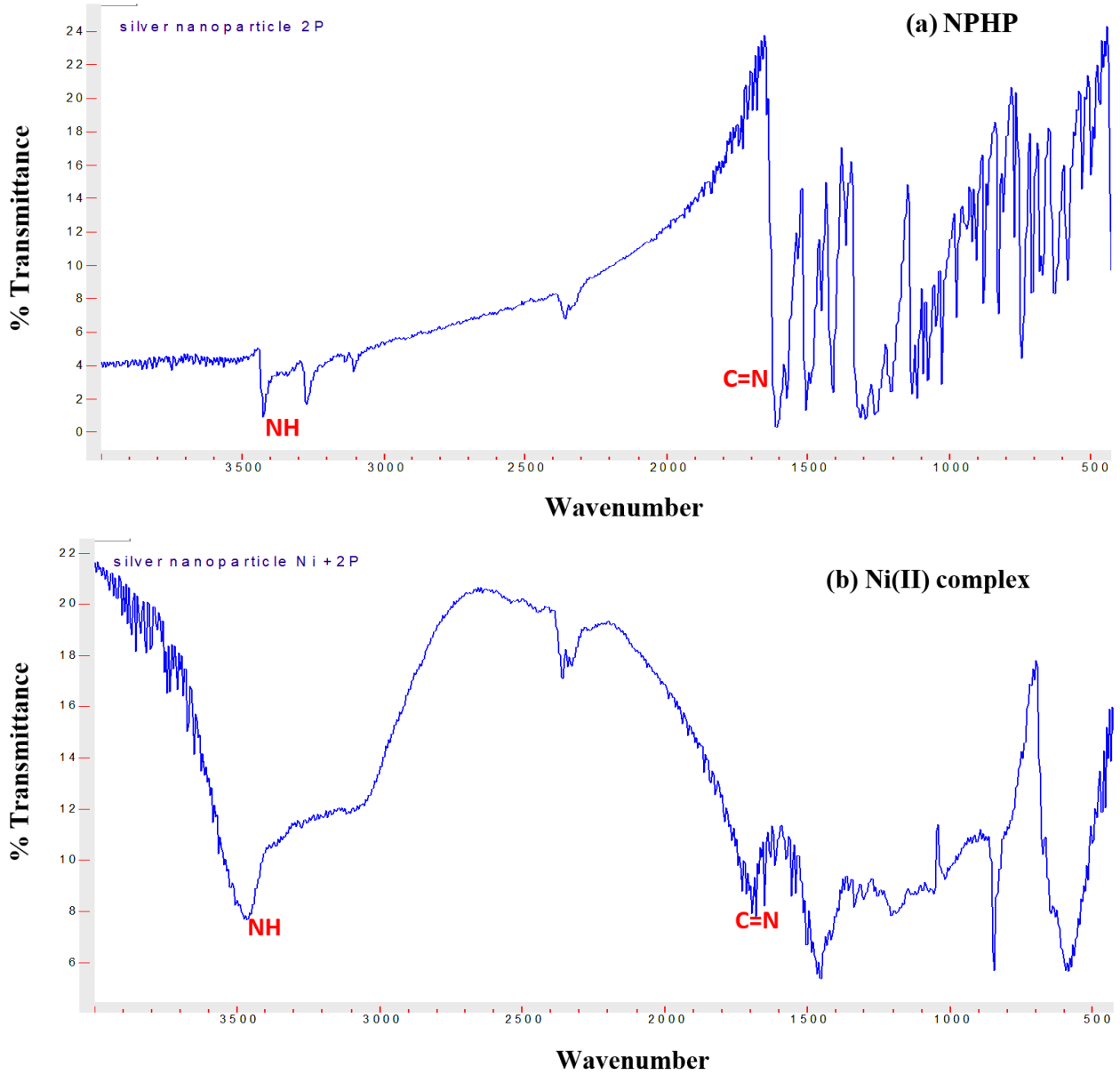

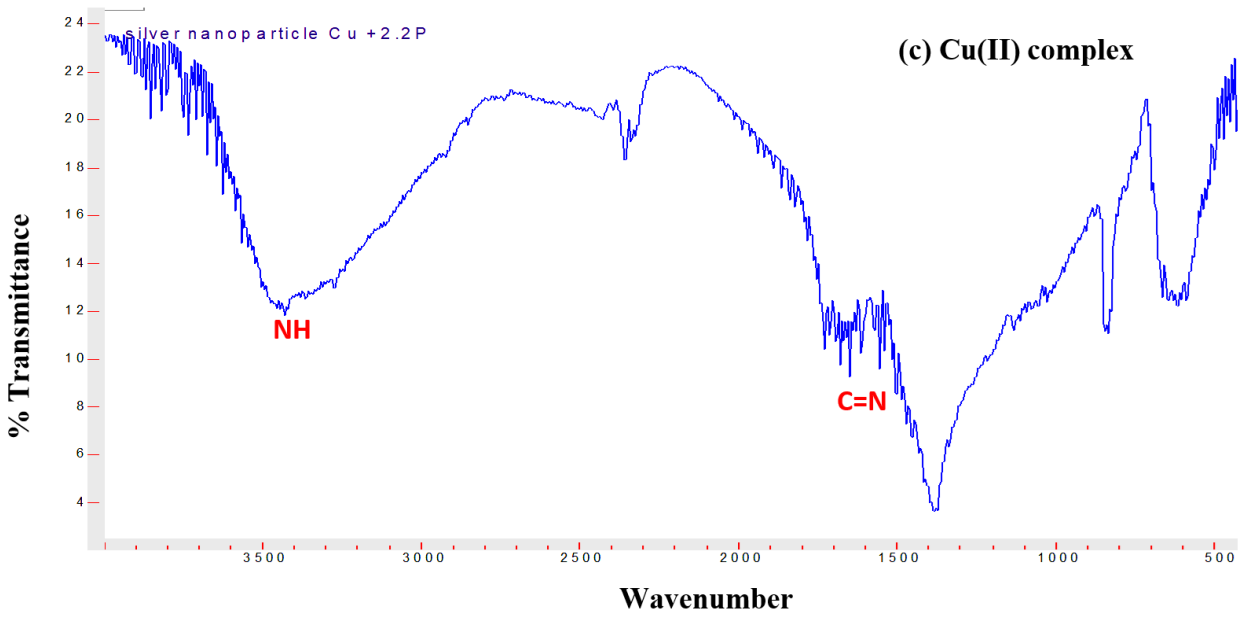


**Figure 1**. FT-IR spectra **(a)** NHPH and **(b)** Ni(II), **(c)** Cu(II) complex.
**Source**: Elaborated by the authors.

## 3.3. UV-Visible spectra

The UV-Visible spectrum of the free ligand NPHP (**Fig. 2a**) shows two notable absorption bands. The first band is observed at 230 nm and 345 nm, corresponding to the π–π* transition of the benzene rings. The second band, located at 345 nm, is attributed to the n–π* transition, which involves non-bonding electrons on the nitrogen atom. These transitions indicate the electronic characteristics of the ligand and provide insights into its molecular structure and behavior in solutions.

In the spectrum of the Ni(II) complex (**Fig. 2b**), also recorded in DMSO, three maxima are observed at 385 nm, 570 nm, and 750 nm. The band at 385 nm is primarily due to intra-ligand charge transfer, while the band at 570 nm is related to metal-ligand charge transfer (MLCT). A broad band at 750 nm is indicative of a d–d transition in the octahedral Ni(II) complex. The spectrum for the Cu(II) complex (**Fig. 2c**), recorded in DMSO, reveals two distinct bands at 420 nm and 550 nm. The band at 420 nm is associated with a metal-to-ligand charge transfer (MLCT) transition, indicating electronic interactions between the metal ion and the ligand. The broad band observed at 550 nm corresponds to a d–d transition in the octahedral Cu(II) complex (Aalami *et al.*, 2024; Gliemann, 1985; Turky Shamkhy, 2015). The absorption band values are summarized in **Table 3**.

**Table 3.** Electronic spectra for prepared compounds.

| Compounds | | NPHP | $Ni^{II}$ complex | $Cu^{II}$ complex |
|---|---|---|---|---|
| λ (nm) | π-π* | 230 | ---- | ---- |
| | n-π* | 345 | ---- | ---- |
| | LMCT | ---- | 385 | ---- |
| | MLCT | ---- | 570 | 420 |
| | d-d | ---- | 750 | 550 |
| Geometry | | ---- | Octahedral | Octahedral |

**Source**: Elaborated by the authors.

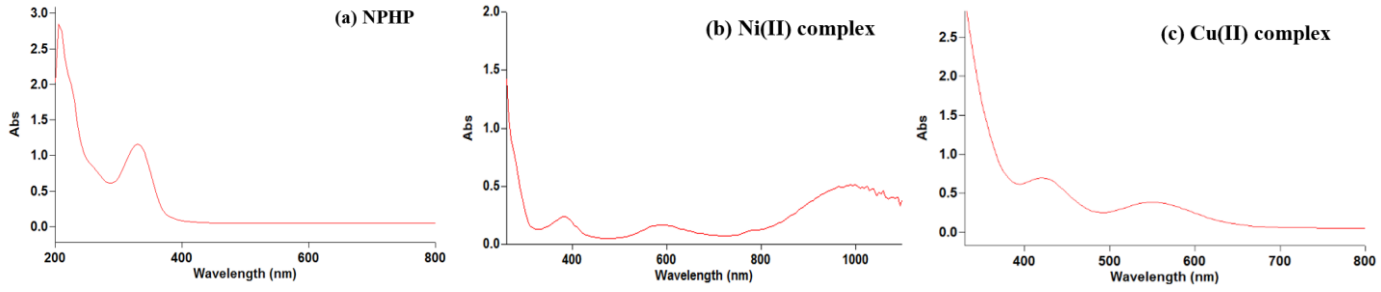


**Figure 2.** UV-Vis spectra of **(a)** NPHP and **(b)** Ni(II), **(c)** Cu(II) complexes.
**Source**: Elaborated by the authors.

## 3.4. XRD analysis

X-ray diffraction (XRD) patterns of NPHP (**Fig. 3a**) were a good match (JCPDS card no. 09-0710). The XRD pattern of the Ni(II)complexes nanoparticles confirms that there are three kinds of phases such as the triclinic (or anorthic) crystalline structure of monoclinic and the small peaks evident for monoclinic (**Fig. 3b**). For Cu(II) complex nanoparticles (JCPDS card no. 50-2456), the monoclinic crystalline structure is excellently represented (**Fig. 3c**). However, impurity peaks were noticed in the XRD pattern, corresponding to JCPDS card no. 08-0564. The diffraction peaks align closely with those listed in the standard JCPDS card No. 35-1877 ($C_{12}H_{12}O_4$), 22-1848 ($C_{10}H_{20}N_4NiO_4$) and 14-0864 ($C_{12}H_{16}N_2CuO_3$). Furthermore, this sample has shown unexpected

X-ray diffraction peaks. NPHP exhibits the largest intensity peaks, whereas Ni(II) complexes nanoparticles display the lowest. The crystallite sizes of the prepared nanoparticles were calculated using Debye-Scherrer's formula (Rathore *et al.*, 2024; Sameeh *et al.*, 2024) (Eq. 1).

$$CapD = \frac{0.9\,\lambda}{\beta\, CoS\, \theta} \quad (1)$$

In this context, λ represents the wavelength of the utilized X-ray, β denotes the full width at half maximum intensity (FWHM) measured in radians, and θ is the diffraction angle. These parameters (Table 4) are commonly used in X-ray diffraction studies to analyze the structural properties of materials, enabling the determination of crystallite size and other characteristics through the Scherrer equation or similar methods. The crystallite sizes (D) for the nanoparticles are as follows: $C_{12}H_{12}O_4$ is 21.2 nm, $C_{10}H_{20}N_4NiO_4$ is 18.3 nm, and $C_{12}H_{16}N_2CuO_3$ is 17.1 nm.

**Table 4.** XRD data for prepared compounds.

| Compounds | hkl | 2-theta (2θ °) | FWHM (β) | D (nm) |
|---|---|---|---|---|
| NPHP | ---- | 26.68 | 0.385 | 21.2 |
| $Ni^{II}$ complex | 021 | 12.26 | 0.437 | 18.3 |
| $Cu^{II}$ complex | 001 | 8.4 | 0.465 | 17.1 |

Source: Elaborated by the authors.

## 3.5. TEM analysis

The Transmission Electron Microscope (TEM) images of the produced samples are presented in Figs. 4 and 5, alongside distribution histograms of the nanoparticles. Particle aggregation was observed, and the TEM images revealed that the particles exhibit spherical and semispherical shapes across all prepared samples. The nanoparticles were within the size range of below 100 nm. The evaluated particle sizes were 31.59 nm for PNHP, 46.80 nm for Ni(II) complexes, and 34.96 nm for Cu(II) complexes.

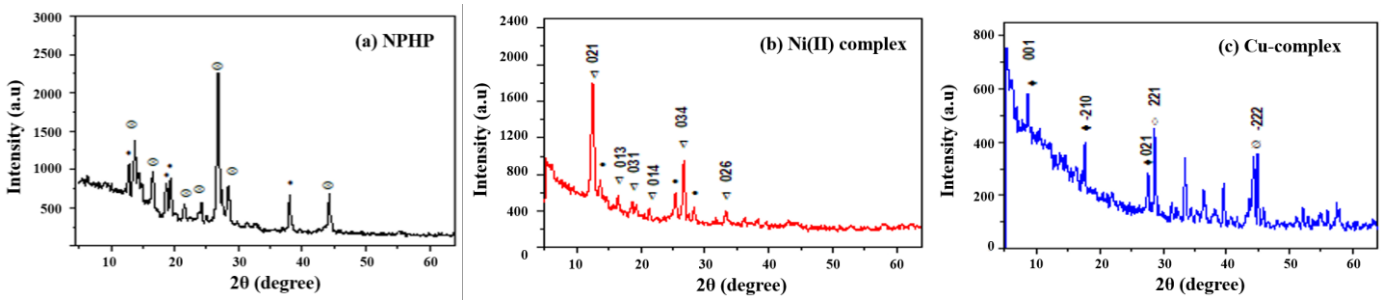


**Figure 3.** XRD pattern of (a) NPHP and (b) Ni(II), (c) Cu(II) complexes.
Source: Elaborated by the authors.

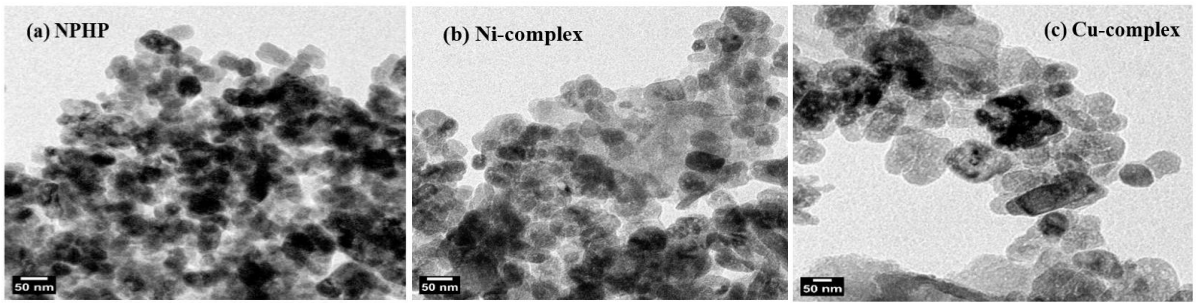


**Figure 4.** TEM images of (a) NPHP and (b) Ni(II), (c) Cu(II) complexes.
Source: Elaborated by the authors.

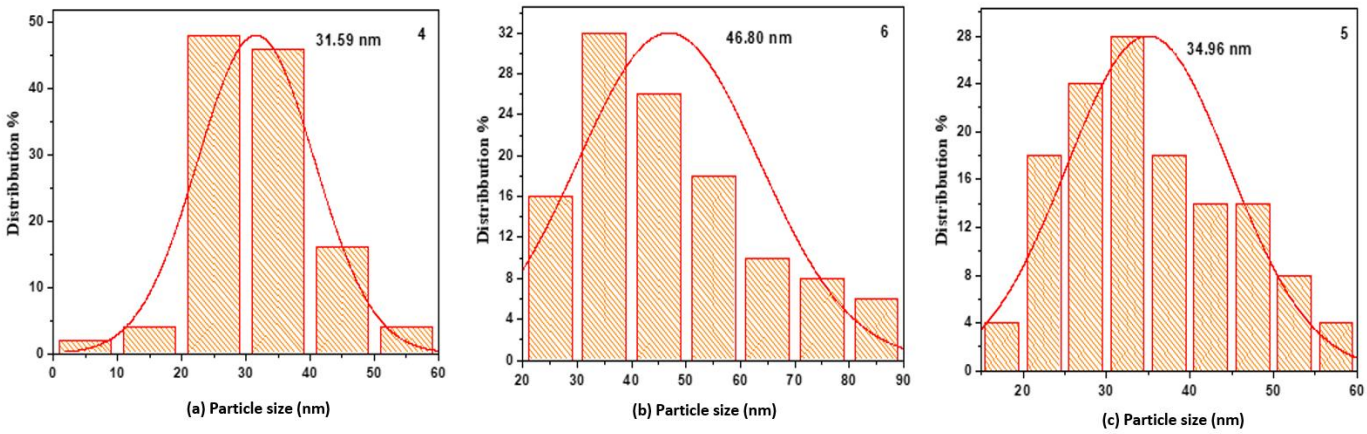


**Figure 5.** TEM distribution particle size of (a) NPHP and (b) Ni(II), (c) Cu(II) complexes.
Source: Elaborated by the authors.

https://doi.org/10.26850/1678-4618.eq.v51.2026.e1621

### 3.6. NMR spectra

NMR spectroscopy is crucial for diagnosing organic molecules, providing significant insights into their chemical composition in solution (Naderi *et al.*, 2023). **Figure 6** presents the $^{1}$H-NMR (DMSO, 300 MHz) δ values in ppm: 8.60 (s, 1H) for the NH of the pyrrole ring; 7.99 - 8.35 (m, 5H) for the benzene ring; 7.10 (m, 3H) for the pyrrole ring; 3.40 (s, 1H) for the NH of the azomethane group; and 2.24 (d, 1H) for the CH=N enamine group, corresponding to the Schiff base ligand (Aranha *et al.*, 2007; Gliemann, 1985; Jailani *et al.*, 2020).

The $^{13}$C-NMR spectrum (**Fig. 7**) of NPHP indicates the presence of nine carbon atoms, consistent with the molecular formula. The δ values in ppm are as follows: 109.70, 112.60, 116.50, and 137.29 for the pyrrole ring; 122.70, 126.90, 136.10, 137.20, and 141.70 for the benzene ring carbon; and 144.50 for the enamine (CH=N) group. The 1H-NMR and 13C-NMR data corroborate the proposed structure of the ligand, as illustrated in **Figs. 6** and **7**.

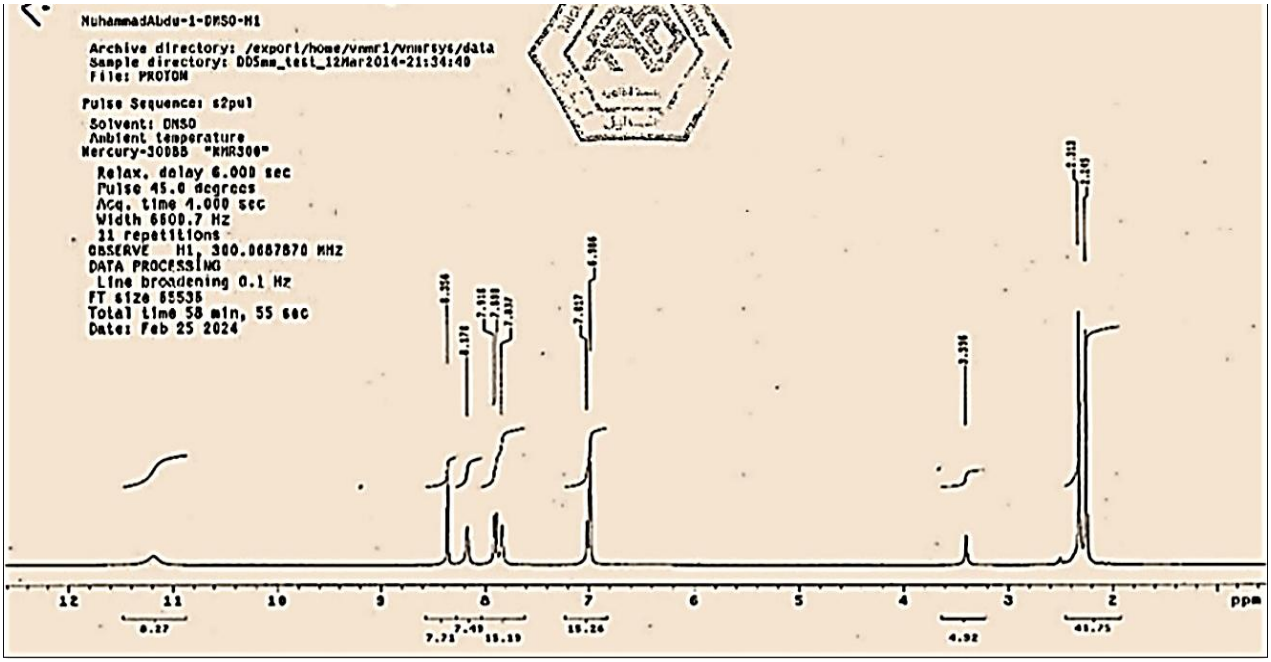


**Figure 6.** $^{1}$HNMR spectrum of the NPHP ligand.
**Source**: Elaborated by the authors.

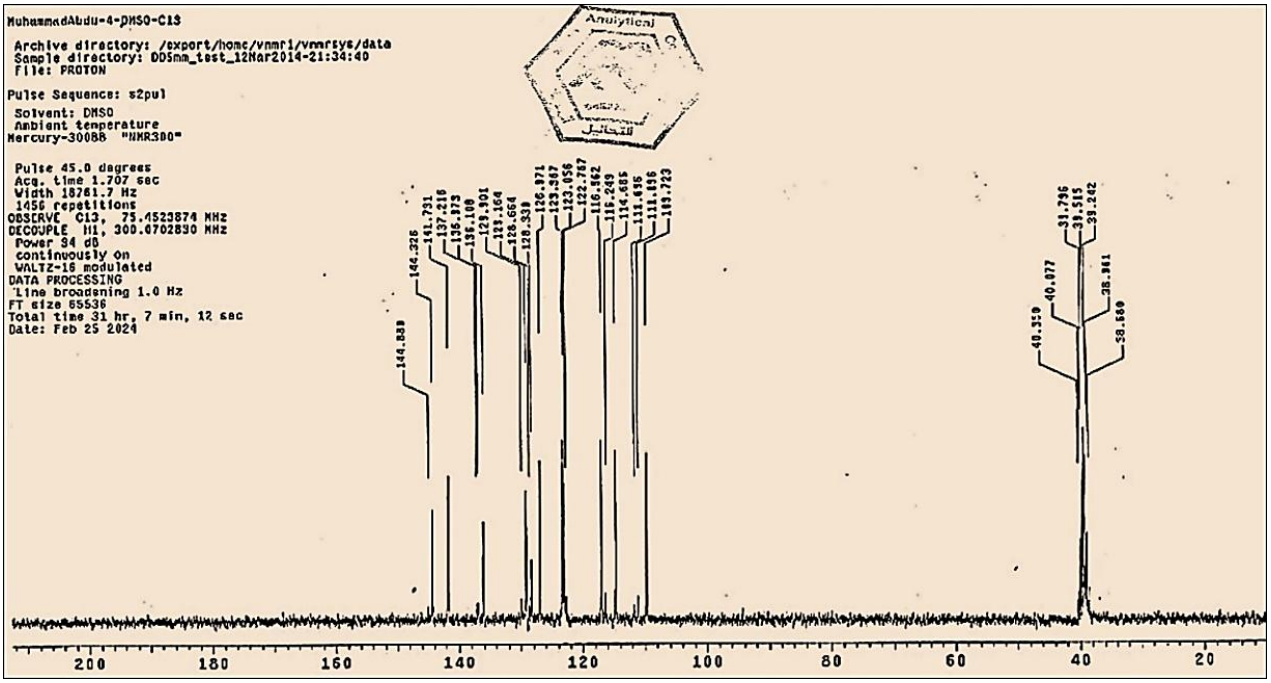


**Figure 7.** $^{13}$CNMR spectrum of the NPHP ligand.
**Source**: Elaborated by the authors.

### 3.7. Antibacterial activity

The antibacterial activity of the Schiff base ligand and its complexes was evaluated at concentrations of 50 and 100 µg/mL against Gram-positive *Staphylococcus aureus* (ATCC 29737), *Pseudomonas aeruginosa* (ATCC 25619), and Gram-negative *Escherichia coli* (ATCC 10536). This evaluation was conducted using the disc diffusion method, which is a standard procedure for assessing antimicrobial activity by measuring the inhibition zones around the discs containing the test compounds (Khan *et al.*, 2020). The results were compared to the antibiotic Ciprofloxacin, with susceptibility zones measured in millimeters (mm) and summarized in **Table 5**.

The items resulting in the highest-to-lowest effectiveness can be summarized as follows:

**a)** *Escherichia coli*
Ciprofloxacin > Ni > Cu

**b)** *Staphylococcus aureus*
Ciprofloxacin > Ni > ligand > Cu

**c)** *Pseudomonas aeruginosa*
Ni > Ciprofloxacin >Cu > ligand

From these results, we can summarize that:

1. Generally, the active property of the antibacterial agent was more active than the ligand and its complexes against *Escherichia coli* and *Staphylococcus aureus*.
2. There is no inhibition zone for the ligand against the *Escherichia coli.*
3. The inhibition zone of the Ni (II) complex against *Pseudomonas aeruginosa* is higher compared to Ciprofloxacin, ligand, and Cu(II) complex.
4. The inhibition zone by complex of Cu (II) complex is less than other compounds against *Escherichia coli* and *Staphylococcus aureus*.

The Ni(II) and Cu(II) complexes showed enhanced activity compared to the NPHP ligand, which is attributed to the formation of metal complexes that rely on the electron-donor properties of the ligand and their accessibility to metal ions. These findings highlight the potential of metal complexes as promising biological agents, surpassing the inhibitory effects of the antibiotic Ciprofloxacin.

**Table 5.** Comparison of the inhibiting activity of synthesized Schiff base ligand and its complexes with antibiotics (inhibiting diameter in mm).

| Compounds | Zone of Inhibition (mm) | | | | | | | | | | | |
|---|---|---|---|---|---|---|---|---|---|---|---|---|
| | *Escherichia coli* | | | | *Staphylococcus aureus* | | | | *Pseudomonas aeruginosa* | | | |
| | Conc. (µg/mL)50 | | Conc. (µg/mL)100 | | Conc. (µg/mL)50 | | Conc. (µg/mL)100 | | Conc. (µg/mL)50 | | Conc. (µg/mL)100 | |
| **Ciprofloxacin** | **20** | | | | **22** | | | | **26** | | | |
| **NPHP** | 0 | 0 | 0 | 0 | 11 | 11 | 18 | 18 | 6 | 6 | 8 | 8 |
| | 0 | | 0 | | 11 | | 18 | | 5.5 | | 8.3 | |
| | 0 | | 0 | | 11 | | 18.5 | | 6 | | 7.8 | |
| **$Ni^{II}$ complex** | 16 | 16 | 18 | 18 | 13 | 13 | 23 | 23 | 14 | 14 | 27 | 27 |
| | 16 | | 18 | | 13 | | 21.5 | | 14 | | 27 | |
| | 17 | | 18 | | 13.5 | | 24 | | 14.5 | | 28 | |
| **$Cu^{II}$ complex** | 11 | 12 | 13 | 13 | 7 | 7 | 24 | 24 | 13 | 13 | 24 | 24 |
| | 12 | | 11.5 | | 6.5 | | 24 | | 12.5 | | 25 | |
| | 12 | | 13.5 | | 7 | | 24.5 | | 12.5 | | 24 | |

**Source**: Elaborated by the authors.

## 4. Conclusions

In this paper, the new Schiff base ligand (NPHP) functions as a bidentate ligand obtained by the condensation reaction of 2,4-dinitrophenyl hydrazine and 1H-pyrrole-2-carbaldehyde with ratio 1:1 gives 2-[(E)-[2-(2,4-dinitrophenyl)hydrazinylidene]methyl]-1H-pyrrole (NPHP), which coordinated with metal ions of Ni(II), and Cu(II) in a 2:1 molar ratio of ligand to metal via the nitrogen donor atoms of azomethine and pyrrole groups is characterized by the physicochemical and spectral analysis for the prepared ligands and complexes have been done. The ligand behaves as bidentate, coordinating via the nitrogen donor atoms of azomethine and pyrrole groups. According to the analytical data, including FT-IR, UV-vis, NMR (1H and 13C), XRD, and TEM, we have proposed an octahedral geometry for Ni(II) and Cu(II) complexes. Furthermore, these metal complexes exhibit enhanced antibacterial activity against Gram-positive *Staphylococcus aureus* (ATCC 29737), Gram-negative *Pseudomonas aeruginosa* (ATCC 25619), and *Escherichia coli* (ATCC 10536) compared to the NPHP ligand and the antibiotic Ciprofloxacin.

## Authors' contribution

**Conceptualization**: Maher Ali Al-Maqtari; Ahmed Ali Qaid; Sadeq Hamood Azzam; **Data curation**: Ahmed Ali Qaid; Amani Ahmed Al-Gaadb; Saad Abdullah Al-Arnoot; **Formal Analysis**: Ahmed Ali Qaid; Bushra Mohammed Alattab; Fares Abdullah Alarbagi; **Funding acquisition**: Not applicable; **Investigation**: Ahmed Ali Qaid; Amani Ahmed Al-Gaadb; Saad Abdullah Al-Arnoot; **Methodology**: Ahmed Ali Qaid; Maher Ali Al-Maqtari; Mohammed Kassem Al-qadasy; **Project administration**: Maher Ali Al-Maqtari; Sadeq Hamood Azzam; **Resources**: Maher Ali Al-Maqtari; Mohammed Kassem Al-qadasy; **Software**: Ahmed Ali Qaid; Fares Abdullah Alarbagi; **Supervision**: Maher Ali Al-Maqtari; Mohammed Kassem Al-qadasy; **Validation**: Sadeq Hamood Azzam; Bushra Mohammed Alattab; Fares Abdullah Alarbagi; **Visualization**: Ahmed Ali Qaid; Saad Abdullah Al-Arnoot; **Writing – original draft**: Ahmed Ali Qaid; Maher Ali Al-Maqtari; Sadeq Hamood Azzam; Amani Ahmed Al-Gaadb; **Writing – review & editing**: Maher Ali Al-Maqtari; Sadeq Hamood Azzam; Mohammed Kassem Al-qadasy.

## Conflict of interest

The authors declare that there is no conflict of interest.

## Data availability statement

All data sets were generated or analyzed in the current study.

## Artificial Intelligence usage statement

The authors declare that they used Gemini (Version 1.5) in the preparation and linguistic improvement of the manuscript's prose to enhance clarity and scientific communication. This tool was used solely for refining the language, grammar, and stylistic structure of the text. All content generated or modified with the assistance of AI was critically reviewed, edited, and validated by the authors to ensure its scientific accuracy, integrity, and compliance with academic standards. The AI tool was not included as an author, nor did it have access to any unpublished raw data or contribute to the core scientific findings of this study.

## Funding

Not applicable.

## Acknowledgments

The authors would like to express their gratitude to Sana'a University, Faculty of Science, Department of Chemistry, for providing the necessary facilities and support to conduct this research. Special thanks are also extended to the Department of Biology for their technical assistance and cooperation.

## References

Aalami, Z.; Hoseinzadeh, M.; Hosseini Manesh, P.; Aalami, A. H.; Es'haghi, Z.; Darroudi, M.; Sahebkar, A.; Hosseini, H. A. Synthesis, Characterization, and Photocatalytic Activities of Green Sol-Gel ZnO Nanoparticles Using Abelmoschus Esculentus and Salvia Officinalis: A Comparative Study versus Co-Precipitation-Synthesized Nanoparticles. *Heliyon*. **2024**, *10* (2), e24212. https://doi.org/10.1016/j.heliyon.2024.e24212

Ahmed, B.; Solanki, B.; Zaidi, A.; Khan, M. S.; Musarrat, J. Bacterial Toxicity of Biomimetic Green Zinc Oxide Nanoantibiotic: Insights into ZnONP Uptake and Nanocolloid–Bacteria Interface. *Toxicol Res.* **2019**, *8* (2), 246–261. https://doi.org/10.1039/C8TX00267C

Alhafez, A.; Savci, A.; Alan, Y.; Söylemez, R.; Kilic, A. Preparation of Cu(II), Ni(II), Ti(IV), VO(IV), and Zn(II) Metal Complexes Derived from Novelvic-Dioxime and Investigation of Their Antioxidant and Antibacterial Activities. *Chem. Biodiversity*. **2022**, *19* (3), e202100768. https://doi.org/10.1002/cbdv.202100768

Al-Maqtari, M. A.; Alattab, B. M.; Qaid, A. A. Biosynthesis of Silver Based Nanoparticles Using Plant Leaves Extracts and Their Antibacterial Activities. *Sana'a Univ. J. Appl. Sci. Technol*. **2023**, *1* (4), 327–338. https://doi.org/10.59628/JAST.V1I4.619

Altammar, K. A. A review on nanoparticles: characteristics, synthesis, applications, and challenges. *Frontiers in Microbiology*. **2023**, *14*, 1155622. https://doi.org/10.3389/fmicb.2023.1155622

Aranha, P. E.; Santos, M. P.; Romera, S.; Dockal, E. R. Synthesis, Characterization, and Spectroscopic Studies of Tetradentate Schiff Base Chromium(III) Complexes. *Polyhedron*. **2007**, *26* (7), 1373–1382. https://doi.org/10.1016/J.POLY.2006.11.005

Al Zoubi, W.; Al-Hamdani, A. A. S.; Kaseem, M. Synthesis and Antioxidant Activities of Schiff Bases and Their Complexes: A Review. *Appl. Organomet. Chem.* **2016**, *30* (10), 810–817. https://doi.org/10.1002/AOC.3506

Bhaskar, R. S.; Ladole, C. A.; Salunkhe, N. G.; Barabde, J. M.; Aswar, A. S. Synthesis, Characterization and Antimicrobial Studies of Novel ONO Donor Hydrazone Schiff Base Complexes with Some Divalent Metal (II) Ions. *Arab. J. Chem*. **2020**, *13* (8), 6559–6567. https://doi.org/10.1016/J.ARABJC.2020.06.012

Ceramella, J.; Iacopetta, D.; Catalano, A.; Cirillo, F.; Lappano, R.; Sinicropi, M. S. A Review on the Antimicrobial Activity of Schiff Bases: Data Collection and Recent Studies. *Antibiotics*. **2022**, *11* (2), 191. https://doi.org/10.3390/ANTIBIOTICS11020191

De, S.; Jain, A.; Barman, P. Recent Advances in the Catalytic Applications of Chiral Schiff-Base Ligands and Metal Complexes in Asymmetric Organic Transformations. *Chemistry Select.* **2022**, *7* (7), e202104334. https://doi.org/10.1002/SLCT.202104334

El-Shafiy, H. F.; Saif, M.; Mashaly, M. M.; Halim, S. A.; Eid, M. F.; Nabeel, A. I.; Fouad, R. New Nano-Complexes of Zn(II), Cu(II), Ni(II) and Co(II) Ions; Spectroscopy, Thermal, Structural Analysis, DFT Calculations and Antimicrobial Activity Application. *J. Mol. Struct.* **2017**, *1147*, 452–461. https://doi.org/10.1016/J.MOLSTRUC.2017.06.121

Gliemann, G. "A. B. P. Lever: Inorganic Electronic Spectroscopy, Vol. 33 aus: Studies in Physical and Theoretical Chemistry, Elsevier, Amsterdam, Oxford, New York, Tokio 1984. 863 Seiten, Preis: $ 113, 50.". *Ber. Bunsenges. Phys. Chem.* **1985**, *89* (1), 99–100. https://doi.org/10.1002/BBPC.19850890122

Hezam, A.; Namratha, K.; Ponnamma, D.; Drmosh, Q. A.; Saeed, A. M. N.; Sadasivuni, K. K.; Byrappa, K. Sunlight-Driven Combustion Synthesis of Defective Metal Oxide Nanostructures with Enhanced Photocatalytic Activity. *ACS Omega*. **2019**, *4* (24), 20595–20605. https://doi.org/10.1021/acsomega.9b02564

Ilhan, S.; Temel, H.; KIIIc, A. Synthesis and spectral studies of macrocyclic Cu(II) complexes by reaction of various diamines, copper(II) perchlorate and 1,4-bis(2-carboxyaldehyde phenoxy)butane. *J. Coord. Chem.* **2008**, *61* (2), 277–284. https://doi.org/10.1080/00958970701327500

Jailani, A. K.; Gowthaman, N. S. K.; Kesavan, M. P. Synthesis, Characterisation and Biological Evaluation of Tyramine Derived Schiff Base Ligand and Its Transition Metal(II) Complexes. *Karbala Int. J. Mod. Sci*. **2020**, *6* (2), 225–234. https://doi.org/10.33640/2405-609X.1637

Kashaw, S. K.; Kashaw, V.; Mishra, P.; Jain, N. K.; Design, synthesis and potential CNS activity of some novel 1-(4-substituted-phenyl)-3-(4-oxo-2-propyl-4H-quinazolin-3-yl)-urea. *General Papers*. **2008** (xiv) 17–26. https://doi.org/10.3998/ark.5550190.0009.e03

Khan, M. M.; Harunsani, M. H.; Tan, A. L.; Hojamberdiev, M.; Azamay, S.; Ahmad, N. Antibacterial Activities of Zinc Oxide and Mn-Doped Zinc Oxide Synthesized Using *Melastoma Malabathricum* (L.) Leaf Extract. *Bioprocess Biosyst. Eng.* **2020**, *43* (8), 1499–1508. https://doi.org/10.1007/S00449-020-02343-3

Kilic, A.; Tas, E.; Deveci, B.; Durgun, M. Dissymmetric tetradentate salicylaldimine Cu(II) and Co(II) complexes derived from 1,8-naphthalene and different salicylaldehydes. *Bulg. Chem. Commun*. **2012**, *44* (4), 289–298.

Kumar, S.; Dhar, D. N.; Saxena, P. N. Applications of Metal Complexes of Schiff Bases-A Review. *J. Sci. Ind. Res.* **2009**, *68* (3), 181–187.

Maher, A. A.; Mohammed, K. A.; Yasmin, M. J.; Fathi, M. A.; Amani, A. A. Physicochemical and biological activity studies on complexes of some transition elements with mixed ligands of glycine and urea. *Eclét. Quím. J.* **2018**, *43* (4), 25–36. https://doi.org/10.26850/1678-4618eqj.v43.4.2018.p25-35

Mushtaq, I.; Ahmad, M.; Saleem, M.; Ahmed, A. Pharmaceutical Significance of Schiff Bases: An Overview. *Future J. Pharm. Sci.* **2024**, *10* (16), 1–12. https://doi.org/10.1186/S43094-024-00594-5

Naderi, S.; Sandaroos, R.; Peiman, S.; Maleki, B. Synthesis and Characterization of a Novel Crowned Schiff Base Ligand Linked to Ionic Liquid and Application of Its Mn(III) Complex in the Epoxidation of Olefins. *Chemical Methodologies.* **2023**, *7* (5), 392–404. https://doi.org/10.22034/chemm.2023.385248.1651

Prabhu, S.; Poulose, E. K. Silver Nanoparticles: Mechanism of Antimicrobial Action, Synthesis, Medical Applications, and Toxicity Effects. *Int. Nano Lett.* **2012**, *2* (1), 1–10. https://doi.org/10.1186/2228-5326-2-32

Ragi, K.; Joby, T. K.; Raphael, V. P.; Johnson, R.; Vidya, K. T. *In Vitro* Antibacterial and in Silico Docking Studies of Two Schiff Bases on *Staphylococcus Aureus* and Its Target Proteins. *Future J. Pharm. Sci*. **2021**, *7* (1), 78. https://doi.org/10.1186/S43094-021-00225-3

Rathore, M. S.; Verma, H.; Akhani, S. B.; Pathak, J.; Joshi, U.; Joshi, A.; Prakash, C.; Kaur, K.; Oza, A. Photoluminescence and Antibacterial Performance of Sol–Gel Synthesized ZnO Nanoparticles. *Mater. Adv.* **2024**, *5* (8), 3472–3481. https://doi.org/10.1039/D3MA01096A

Sameeh, M.; Khairy, M.; Mousa, M. A. Structural, Optical, Electrochemical, and Ion Transference Characteristics of the PVA-Based Plasticized Polymer Composite Electrolyte: LiI Doped with Plasticizer (D-Sorbitol). *Ionics*. **2024**, *30* (11), 7097–7112. https://doi.org/10.1007/S11581-024-05788-8

Shivankar, V. S.; Vaidya, R. B.; Dharwadkar, S. R.; Thakkar, N. V. Synthesis, Characterization, and Biological Activity of Mixed Ligand Co(II) Complexes of 8-Hydroxyquinoline and Some Amino Acids. *Synth. React. Inorg. Met.-Org. Chem.* **2003**, *33* (9), 1597–1622. https://doi.org/10.1081/SIM-120025443

Suman, G. R.; Bubbly, S. G.; Gudennavar, S. B.; Muthu, S.; Roopashree, B.; Gayatri, V.; Nanje Gowda, N. M. Structural Investigation, Spectroscopic and Energy Level Studies of Schiff Base: 2-[(3′-N-Salicylidenephenyl)Benzimidazole] Using Experimental and DFT Methods. *J. Mol. Struct.* **2017**, *1139*, 247–254. https://doi.org/10.1016/j.molstruc.2017.03.043

Turky Shamkhy, E. Synthesis, Characterization and Spectroscopic Studies of 2-{(E)-Hydroxyphenyl)Imino]Methyl}Phenol Schiff Base with Some Metal Complexes. *J. Al-Nahrain Univ.* **2015**, *18* (1), 39–45. https://doi.org/10.22401/JNUS.18.1.05

Yilmaz, I.; Ilhan, S.; Temel, H.; Kilic, A. Synthesis, characterization and electro-spectroelectrochemical studies of four macrocyclic Schiff-base Co(II) complexes having $N_2O_2$ set of donor atoms. *J. Incl. Phenom. Macrocycl. Chem.* **2009**, *63*, 163–169. https://doi.org/10.1007/s10847-008-9502-9

Yousif, E.; Majeed, A.; Al-Sammarrae, K.; Salih, N.; Salimon, J.; Abdullah, B. Metal Complexes of Schiff Base: Preparation, Characterization and Antibacterial Activity. *Arab. J. Chem*. **2017**, *10*, S1639–S1644. https://doi.org/10.1016/J.ARABJC.2013.06.006